IOPscience iopscience.iop.org

Home Search Collections Journals About Contact us My IOPscience

The LC resonance probe for determining local plasma density

This article has been downloaded from IOPscience. Please scroll down to see the full text article.

2011 Plasma Sources Sci. Technol. 20 025003

(http://iopscience.iop.org/0963-0252/20/2/025003)

View the table of contents for this issue, or go to the journal homepage for more

Download details:
IP Address: 132.250.22.5
The article was downloaded on 18/02/2011 at 21:10

Please note that terms and conditions apply.

Plasma Sources Sci. Technol. **20** (2011) 025003 (7pp) doi:10.1088/0963-0252/20/2/025003

The LC resonance probe for determining local plasma density

D R Boris, R F Fernsler and S G Walton

Naval Research Laboratory, Charge Particle Physics Branch–Code 6752, Plasma Physics Division, 4555 Overlook Ave. SW, Washington, DC 20375, USA

E-mail: david.boris.ctr@nrl.navy.mil

Received 8 September 2010, in final form 10 December 2010
Published 17 February 2011
Online at stacks.iop.org/PSST/20/025003

Abstract

We present a novel plasma diagnostic for measuring local plasma density in reactive-gas plasmas, and depositing plasmas. The diagnostic uses a network analyzer to measure the LC resonance (LCR) frequency of a parallel plate capacitor with inductive leads. The location of the LCR (ω_R) in frequency space is then used as a measure of the plasma dielectric constant ε_p between the plates. By properly constructing the LCR probe, ω_R can be tuned such that $\omega_R \gg \omega_{ce}$, where ω_{ce} is the electron-cyclotron frequency. Thus, the probe can be used in plasmas with varying degrees of magnetization while avoiding complications introduced to ε_p when ω is comparable to ω_{ce}. Density measurements from the LCR probe are compared with Langmuir probe measurements in an electron-beam generated plasma in which density varied from 10^9 to 10^{11} cm^{-3}. An axial magnetic field, typically used to confine the electron beam, was varied between 0 to 300 G. The LCR probe showed good agreement with a Langmuir probe across the entire range of magnetic fields.

(Some figures in this article are in colour only in the electronic version)

1. Introduction

In plasma processing systems, density measurements are an integral part of the parametrization of plasma sources. The most common diagnostic for this measurement is the Langmuir probe, which uses changes in charged particle flux as a function of applied voltage as a measure of the dc plasma resistance [1]. In spite of their common usage Langmuir probes are of limited utility in a number of plasma processing environments. These include depositing plasmas, such as those produced by magnetron discharges, and reactive-gas plasmas. In these cases, the probe surface is modified rendering the probe ineffectual. More specifically, changes to the probe surface area and the deposition of insulating material change the measured surface current. An attractive and widely used alternative to Langmuir probes in these scenarios are RF probe techniques [2–10] since they are unaffected by changes to the probe surface either through deposition or erosion. The LC resonance (LCR) probe, or simply LCR probe, is a variant of the RF probe. The LCR probe is constructed by terminating a semi-rigid coaxial cable with a small capacitor consisting of two parallel metallic plates, one connected to the center conductor and the other to the outer shield of semi-rigid coaxial cable. This configuration provides an LC circuit with a characteristic resonance frequency ω_{R0}, which can be measured with a network analyzer. The shift of this resonant frequency in the presence of a plasma can be used to determine the plasma density.

Importantly, the LCR probe has an advantage over antenna-based RF probes when a magnetic field is present. Simple antenna-based RF probes are unable to measure the plasma frequency directly when a magnetic field is present. Instead, the upper hybrid frequency is measured requiring accurate knowledge of the local magnetic structure for plasma density to be calculated [11, 12]. If the LCR probe is properly constructed, ω_R can be tuned such that $\omega_R \gg \omega_{ce}$, where ω_{ce} is the electron-cyclotron frequency. In this frequency range the plasma dielectric constant, ε_p (ω), is not significantly affected by the magnetic field. Thus, the LCR probe can make plasma density measurements in magnetized plasmas without having to compensate for magnetic field effects. This is similar to the operation of the hairpin resonator [13] which measures plasma density by noting the shift in the structural resonance of a U-shaped wire. The LCR probe, however, differs from the

 © 2011 IOP Publishing Ltd Printed in the UK & the USA

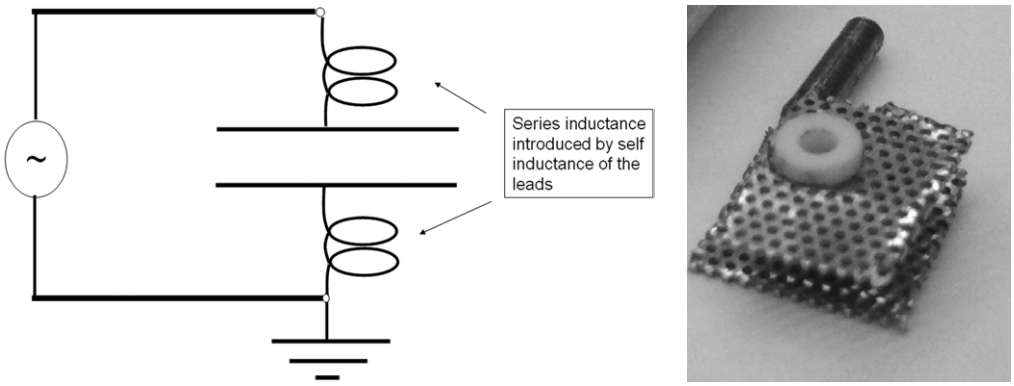

Figure 1. Equivalent circuit for a non-resistive object of size $d \ll c/\omega$. To the right is an image of a 1 cm^2 parallel plate LCR probe with a 2.5 mm plate spacing. The plates are electrically separated by a ceramic spacer.

hairpin resonator in that it does not require a standing wave to be present between the plates. This allows the LCR probe to access lower plasma densities than would be possible with a hairpin resonator.

The spatial resolution of the LCR probe is ultimately limited by the separation distance between the two plates. This is particularly useful for electron-beam generated plasmas in which the beam produces a well-defined ionization volume with large plasma density gradients outside the beam. Antenna-based RF probe measurements in these environments have been shown to be difficult to interpret [14]. In these experiments the plate separation was 2.5 mm (see figure 1).

2. Principles of LCR probe operation

The LCR probe is based on the following principle: any short ($l \ll \lambda$ where l is the characteristic length scale of the probe), non-resistive object can be represented as capacitive and inductive elements in series, as illustrated in figure 1. The capacitive components C account for charge stored on the object and dominate at low frequency. The inductive components L account for current flowing through the object and dominate at high frequency. At the resonance frequency ω_R, the two effects cancel such that the total impedance,

$$Z = \mathrm{i}\omega L + \frac{1}{\mathrm{i}\omega C}, \tag{1}$$

is zero, and therefore

$$\omega_R = \frac{1}{\sqrt{LC}}. \tag{2}$$

For two closely spaced parallel plates, the capacitance is given by

$$C = \frac{A\varepsilon\varepsilon_0}{d} \tag{3}$$

where A is the plate area, ε_0 is the vacuum permittivity, ε is the relative dielectric constant of the medium between the plates and d is the separation distance between the plates. For free space $\varepsilon = 1$. Thus, for the circuit in figure 1, the LCR frequency can be expressed as

$$\omega_R = \left(\frac{d}{LA\varepsilon\varepsilon_0}\right)^{1/2}. \tag{4}$$

Note the importance of ensuring that $d \ll A^{1/2}$ to minimize fringing fields and coupling to other experimental components. Also, the parallel plates should be kept far from other grounded electrodes in the experimental system; however, if the measurements can be performed with both plates electrically isolated from the vacuum vessel then these constraints can be relaxed.

Immersing the parallel plate capacitor in a plasma produces a shift in the LCR frequency. This shift is due to the change in the relative dielectric constant between the parallel plates that occurs when the plasma is introduced. The new ε will be defined by the cold plasma dielectric tensor [15], ε_p:

$$\varepsilon_p = \begin{pmatrix} S & -iD & 0 \\ iD & S & 0 \\ 0 & 0 & P \end{pmatrix}, \tag{5}$$

where

$$S = 1 - \frac{\omega_{pe}^2}{\omega^2 - \omega_{ce}^2}, \tag{5a}$$

$$D = \frac{\omega_{ce}\omega_{pe}^2}{\omega(\omega^2 - \omega_{ce}^2)} \tag{5b}$$

and

$$P = 1 - \frac{\omega_{pe}^2}{\omega^2}. \tag{5c}$$

Here ω_{pe} is the local electron plasma frequency, ω_{ce} is the electron-cyclotron frequency and the magnetic field B is assumed to be along z. While ε_p is a tensor, it can be made to act like a scalar by constructing the probe such that the LC resonant frequency in the absence of plasma obeys the constraint

$$\omega_{R0} = \sqrt{\frac{d}{LA\varepsilon_0}} \gg \omega_{ce}, \omega_{pe}. \tag{6}$$

In this case $S \to P$, $D \to 0$ and ε_p reduces to

$$\varepsilon_p = \left(1 - \frac{\omega_{pe}^2}{\omega^2}\right) \boldsymbol{I}, \tag{7}$$

where $\boldsymbol{I}$ is the identity tensor and the electron plasma frequency is given by

$$\omega_{pe} = \left(\frac{e^2 n_e}{\varepsilon_0 m_e}\right)^{1/2}. \tag{8}$$

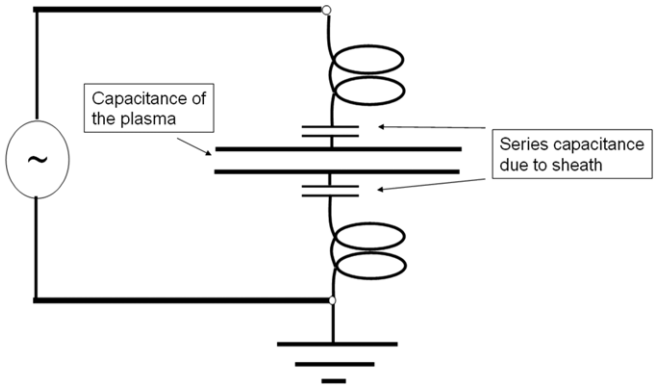

Figure 2. Equivalent circuit modified by the presence of plasma sheaths around the capacitor plates.

Here e is the electron charge and m_e is the electron mass. Using equations (4), (6) and (7), one can readily show the electron density can be determined from the change in resonant frequency ω_{R0} without plasma to the resonant frequency ω_R with plasma as follows:

$$n_e = \frac{m_e \varepsilon_0}{e^2}(\omega_R^2 - \omega_{R0}^2). \tag{9}$$

2.1. Vacuum sheath correction

Equation (9) is derived assuming that the plasma uniformly fills the entire volume between the parallel plates of the LCR probe. This, however, is not the case since the plasma will develop sheaths at the surfaces of both plates. A simple correction is to approximate the sheaths as vacuum regions between the plate surfaces and the bulk plasma. While this is a crude approximation [16] it is adequate for estimating the degree to which sheath effects will perturb the plasma density measurements. The total capacitance of the system, C_T, can then be approximated as the capacitance of the plasma, C_p, as well as the capacitances of the sheaths, C_s, at the surface of the two plates (see figure 2) where

$$C_s = \frac{A\varepsilon_0}{s}, \tag{10}$$

$$C_p = \frac{A\varepsilon_p \varepsilon}{d - 2s} \tag{11}$$

and

$$C_T = \frac{C_p C_s}{C_s + 2C_p}. \tag{12}$$

This implies that ω_R in the presence of a plasma can be expressed as

$$\omega_R^2 = \frac{d - 2s(\omega_{pe}^2/\omega_R^2)}{LA\varepsilon_0\, \varepsilon_p|_{\omega\to\omega_R}}. \tag{13}$$

This expression can be solved for ω_{pe} to yield the following relation for plasma density, corrected for the presence of vacuum sheaths at the plate surfaces:

$$n_e = \frac{m_e \varepsilon_0}{e^2}\left(\frac{\omega_R^2 - \omega_{R0}^2}{1 - (2s/d)(\omega_{R0}/\omega_R)^2}\right). \tag{14}$$

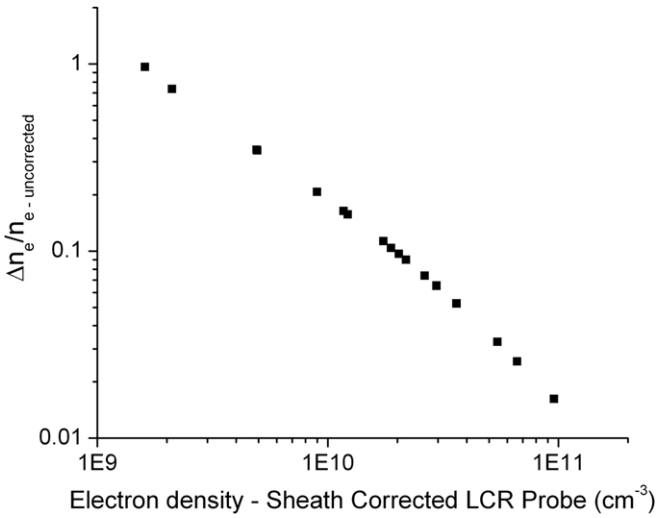

Figure 3. The magnitude of the sheath correction as a function density over a variety of plasma conditions. The sheath correction (equation (15)) results in 100% increase in the calculated density at 2×10^9 cm^{-3} and a 2% increase in calculated density at 10^{11} cm^{-3}.

Like equation (9), equation (14) provides a means for calculating the electron density n_e from the frequency shift in the LCR induced by the plasma. However, equation (14) also takes into account the sheaths around each plate. For example, assume $s = \alpha\lambda_D$, where s is the sheath thickness and λ_D is the electron Debye length. The parameter α depends on the probe voltage and is typically ~5 for a floating probe. Setting $\lambda_D = (\varepsilon_0 T_e/e^2 n_e)^{1/2}$ where T_e is the electron temperature, equation (14) becomes a quadratic for $\sqrt{n_e}$ with solution

$$\sqrt{n_e} = \frac{\alpha}{d}\sqrt{\frac{\varepsilon_0 T_e}{e^2}}\left(\frac{\omega_{R0}}{\omega_R}\right)^2 + \sqrt{\frac{\alpha^2}{d^2}\frac{\varepsilon_0 T_e}{e^2}\left(\frac{\omega_{R0}}{\omega_R}\right)^4 + \frac{m_e\varepsilon_0}{e^2}(\omega_R^2 - \omega_{R0}^2)} = 0. \tag{15}$$

This equation gives n_e in terms of α, T_e, d, ω_{R0} and ω_R, with α, T_e and d being specified *a priori*. For the results given later, we assumed $\alpha = 5$ and $T_e = 0.5$ eV, the latter being typical for plasmas produced by electron beams [20]. It should be noted that frequency probes can be also used to measure T_e, as described by Walker *et al* [17]. This provides an explicit measurement of T_e in environments where a Langmuir probe is impractical, and in that case only α and d need to be specified. The magnitude of vacuum sheath correction as a function of density is shown in figure 3, where a large sampling of data points is presented to show the effect of equation (15) on uncorrected data for a variety of plasma conditions.

3. Experimental setup

The experiments were performed in the electron-beam generated plasma processing chamber at the Naval Research Laboratory [18, 19]. The processing system consists of a large, rectangular, stainless steel, vacuum vessel (width 120 cm, height 55 cm and length 120 cm). Within the vacuum vessel are the following: the electron-beam source, provided by Sigma

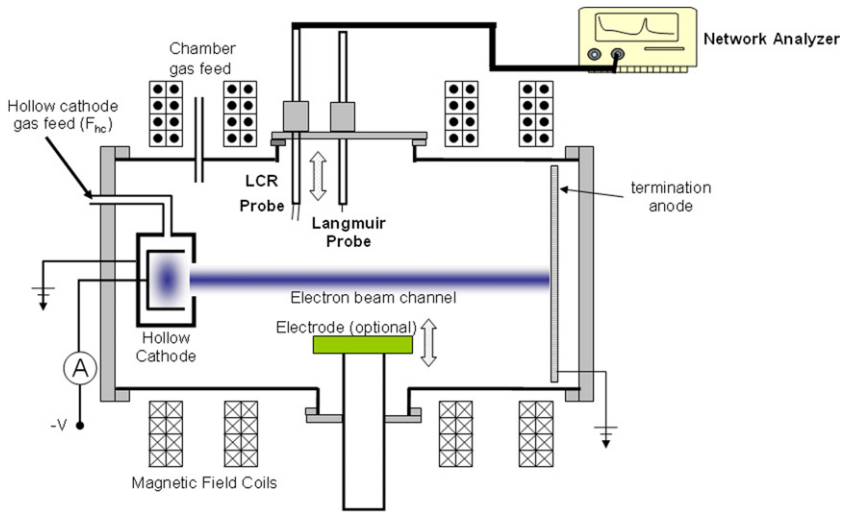

Figure 4. Diagram of the electron-beam plasma processing chamber showing a plasma diagnostic configuration consisting of the LCR probe and a Langmuir probe.

Technologies International Inc., a movable processing stage, a termination anode for the electron beam, a Langmuir probe and an LCR probe diagnostics. Along the length of the chamber are magnetic field coils that produce a uniform axial magnetic field within the vacuum chamber, a diagram of which is shown in figure 4.

The electron source consists of a linear cathode enclosed in a grounded rectangular box with a 1 cm slot located opposite the cathode, and is capable of providing a sheet-like, high energy electron beam with energies as large as 5 keV. When a negative high voltage is applied to the linear cathode a high density, dc glow discharge plasma is formed within the source. The electrons emitted from the cathode (via ion impact) are accelerated across the high-voltage cathode sheath, producing the high energy beam that propagates through the slot. The magnetic field confines the beam electrons to a sheet geometry creating a similarly shaped plasma.

The LCR probe consists of a capacitive element with inductive connections to a length of rigid coaxial cable. The rigid coax, when used in conjunction with a linear motion vacuum feedthrough, provides ≈20 cm range of motion within the vacuum vessel which allowed the probe to sample both above and below the electron beam. The capacitive element consists of two small stainless steel plates (each ≈1 cm^2) separated by a 3 mm gap. One plate is electrically connected to the center conductor of the rigid coaxial cable while the other plate is connected to the grounded outer shield. The plates can be constructed from either solid sheets of metal or from a metallic mesh, provided that the hole size of the mesh is much smaller than the wavelength of the RF signal being generated by the network analyzer. A mesh is advantageous in electron-beam generated plasmas as it allows the electron beam to be transmitted through the probe when oriented perpendicular to the beam. The length and geometry of the connections between the capacitive element of the probe and the rigid coax allow for some control over the inductance of the LCR probe, which provides some control of the location (in frequency space) of the LCR, ω_{R0}. The geometry of the capacitive element of the LCR probe can also be adjusted to tune the location of the LCR. The rigid coax is then connected to an HP 8753D Network Analyzer through a 50 Ω, RG 303 coaxial cable.

When connected to the network analyzer the complex reflection coefficient, Γ, is measured and the impedance of the system calculated according to

$$Z = Z_0 \frac{1+\Gamma}{1-\Gamma} \tag{16}$$

where Z_0 is the analyzer's internal impedance of 50 Ω. This measurement technique relies on the user's ability to properly calibrate the probe to eliminate stray capacitances and inductances. This is done by building a matched 50 Ω load, an electrical short and open termination which are calibrated to provide Γ values of 0, −1 and 1, respectively. This allows stray capacitance from the cabling and other components to be eliminated. References [5, 7] explain this procedure in detail. In practice, the length of rigid coax and coaxial cable should be minimized so as to minimize the inductance and capacitance introduced by these components.

Once calibration is completed, the network analyzer can properly measure the location of the LCR associated with the LCR probe. The resonance is marked by two distinguishing features: (i) a minimum in the frequency-dependent impedance measured by the network analyzer; and (ii) a jump in phase angle from −90° to +90° as the impedance changes from capacitive to inductive. Both features are evident in figure 5, with and without plasma, and the jump in phase angle makes the resonant frequencies especially easy to determine.

Measurements by the LCR probe are benchmarked by a heated cylindrical Langmuir probe, with electron density calculated from the electron current at V_p, the plasma potential. The Langmuir probe consists of a thin loop of wire 3 mm in length with a collection area of 1.5×10^{-2} cm^2. The diagnostic and data acquisition routines follow those previously discussed [20]. Like the LCR probe, the Langmuir probe is mounted to the top of the vacuum chamber with a linear motion feedthrough that allows ≈20 cm of motion through the vacuum vessel, perpendicular to the beam axis.

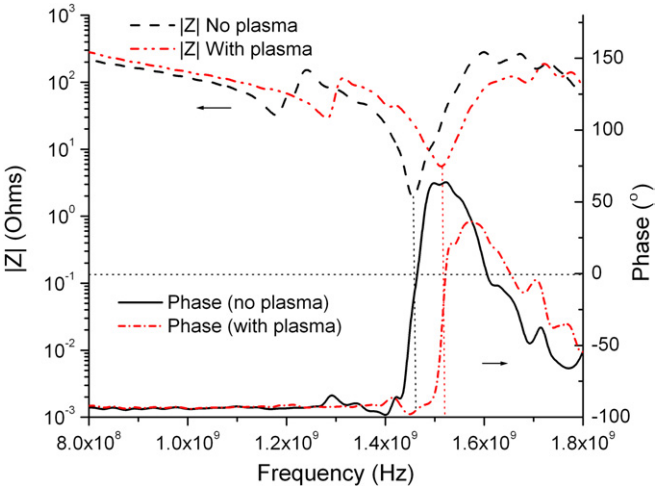

Figure 5. The magnitude of the LCR probe impedance plotted with the phase shift between outgoing and reflected power as a function of frequency. The LCR, f_R, without plasma is clearly visible at 1.47 GHz. In the presence of a 3.5×10^9 cm^{-3} plasma f_R shifts to 1.52 GHz.

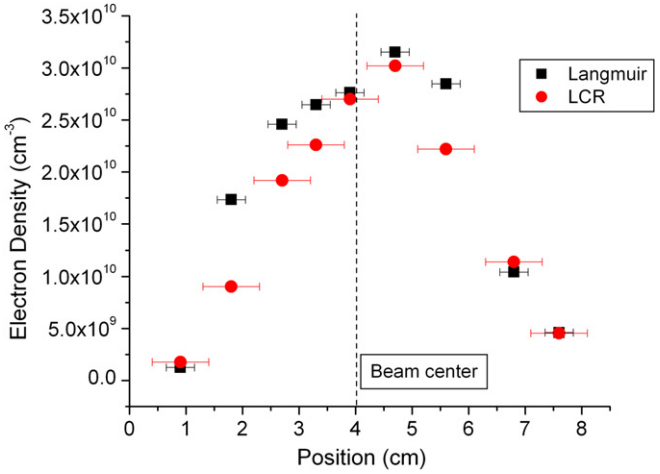

Figure 6. Plasma density profile measurement made with LCR probe and Langmuir probe. 30% transparent stainless steel mesh capacitor plates were used with $E_{ac} \perp B$ (where E_{ac} is the ac electric field between the plates). LCR probe data employed the equation (15) sheath correction. (Profile taken in argon at 10 mTorr with a 1 kV cathode voltage). The position uncertainty was ±0.5 cm and ±0.25 cm for the LCR and Langmuir probes, respectively.

4. Results and discussion

The ability to make local density measurements in highly non-uniform plasmas with the LCR probe is illustrated in figure 6, which shows a density profile for an electron-beam generated plasma measured by both the LCR probe and a Langmuir probe. The uncertainty in the location of the density measurement is noted by the x-axis error bars in the figure. The Langmuir probe and LCR probe are in very good agreement throughout the density profile, with the electron densities measured by the two diagnostics generally differing by less than 40%. A possible source of the slightly higher density measured by the Langmuir probe, within the electron beam, could be due to secondary electron production from

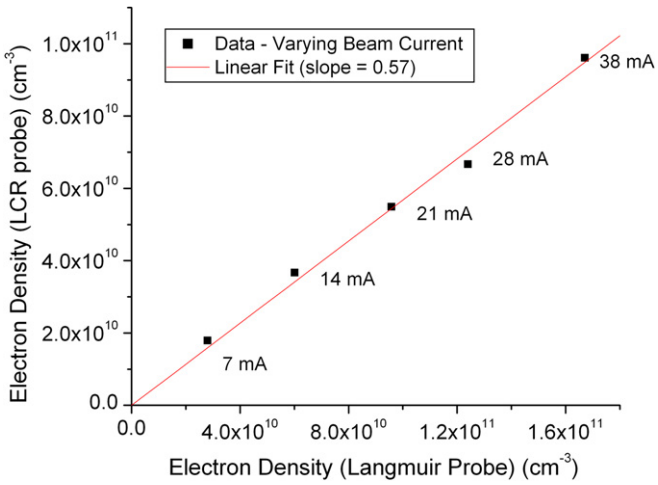

Figure 7. A comparison between Langmuir probe density measurements and LCR probe density measurements. The beam current was varied to change the density. Beam currents are labeled in the figure. All measurements were performed with 10 mTorr of argon fill gas and an axial magnetic field of 100 G.

high energy electrons striking the Langmuir probe surface and ceramic probe stalk. The metallic surface area of the Langmuir probe exposed to the beam is very small so secondary emission from the ceramic is likely to be the main contributor to any excess collected current by the probe. Ceramics are known to have secondary emission coefficients of 5–10, and thus the stalk could be a significant source of low energy electrons [21]. If so, the LCR probe is more likely to provide an accurate measure of n_e, since particle flux is irrelevant. Note also that the LCR probe is equally insensitive to surface contamination, ion currents, plasma drift and low-density electron beams. Moreover, the LCR resonance is sharp and well defined, the LCR analysis is straightforward (no fitting of data to an assumed curve), and magnetic effects can either be incorporated or overcome.

The LCR probe was also compared with Langmuir probe measurements for varying experimental parameters such as electron-beam current (figure 7) and axial magnetic field (figure 8). Here again, the LCR probe showed good agreement with the Langmuir probe. The LCR probe and Langmuir probe measurements were taken 1 cm above the electron beam to eliminate any complications from the electron beam impacting the Langmuir probe. In figure 7 the LCR probe data was acquired using mesh plates as the capacitive element and is presented with the vacuum sheath correction. For the data shown in figure 6, the ratio s/d varied between 0.02 and 0.08, assuming $\alpha = 5$. As an additional check on the plasma density, one can compute n_e from a maximum in Re$[Z(\omega)]$ at either ω_{pe} or $\omega_{uh} = (\omega_{pe}^2 + \omega_{ce})^{1/2}$, depending on the orientation of the probe relative to the applied magnetic field, this technique is described in detail in [5, 7].

The magnetic field scan in figure 8 illustrates how the LCR probe is able to measure plasma density without being substantially affected by the presence of a magnetic field. In this case the ac electric field was oriented perpendicular to the magnetic field axis, and the two plates consisted of metallic mesh. In this orientation the magnetic field has no effect on

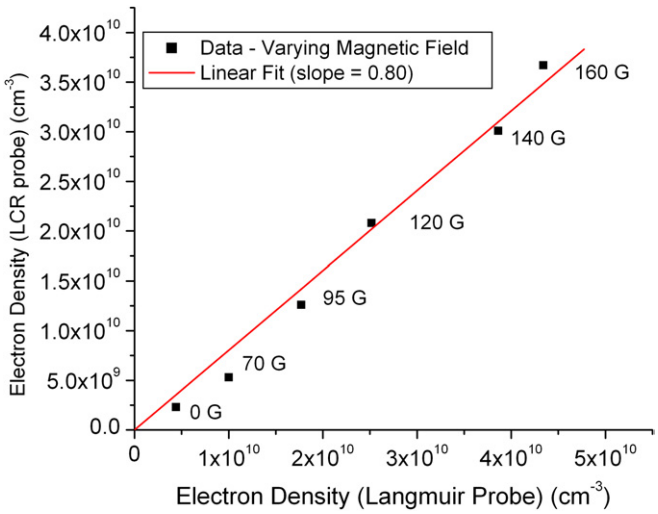

Figure 8. A comparison of Langmuir probe density measurements and LCR probe density measurements for varying applied magnetic field B. The electron-cyclotron frequencies for the 70 G and 160 G magnetic fields are 196 MHz and 448 MHz, respectively. These data were taken with E_{ac} perpendicular to B.

Table 1. Comparison of perpendicular and parallel ac electric field orientations relative to the magnetic field axis. Experimental conditions were as follows: magnetic field = 150 G, pressure = 21 mTorr (argon), cathode voltage = 2500 V.

	n_e (cm^{-3}) (LCR probe with sheath correction)	ω_R (rad s^{-1})	ω_{R0} (rad s^{-1})	n_e (cm^{-3}) (Langmuir probe)
$E_{ac} \perp B$	5.6×10^{10}	1.23×10^{10}	9.16×10^{9}	7.7×10^{10}
$E_{ac} \parallel B$	5.2×10^{10}	1.21×10^{10}	9.16×10^{9}	7.0×10^{10}

ε_p, and good agreement between LCR probe and Langmuir probe was obtained even at magnetic fields as high as 160 G.

The magnetic field has the greatest effect on ε_p when B is perpendicular to the ac electric field E_{ac}, and table 1 compares results obtained for n_e in this configuration with those obtained when $B \parallel E_{ac}$. The two orientations gave essentially the same result for n_e when normalized to the density inferred from the Langmuir probe, showing that the technique is insensitive to the magnetic field. The slight differences reflect typical plasma density fluctuations for this system.

5. Conclusions

In this work an LCR probe was used to determine the local electron density n_e in magnetically confined, electron-beam generated plasmas. The results for n_e agreed well with those obtained using a Langmuir probe, at densities ranging from 10^9 to 10^{11} cm^{-3}. Unlike other RF probes, the LCR probe was shown to work well even in the presence of the moderate (50–200 G) magnetic fields commonly used in electron-beam generated plasmas. These characteristics make LCR probes a viable alternative to Langmuir probes, especially in situations where the surface of the probe is likely to be altered by the plasma environment. Since the probe can be constructed to have a resonant frequency unaffected by the magnetic field, it should be equally useful for space plasmas where the orientation of the magnetic field with respect to the probe varies with time and is often unknown.

Acknowledgments

This work has been supported by the Office of Naval Research. This research was performed while the author, D R Boris, held a National Research Council Research Associateship Award at the Naval Research Laboratory. The authors also acknowledge the valued expertise of Drs Dave Walker and Dave Blackwell.

References

[1] Hershkowitz N 1989 *Plasma Diagnostics* vol I (New York: Academic) p 113
[2] Harp R S and Crawford F W 1964 Characteristics of the Plasma Resonance Probe *J. Appl. Phys.* **35** 3436
[3] Shirakawa T and Sugai H 1993 Plasma oscillation method for measurements of absolute electron density in a plasma *Japan. J. Appl. Phys.* **32** 5129
[4] Stenzel R L 1976 Microwave resonator probe for localized density measurements in weakly magnetized plasmas *Rev. Sci. Instrum.* **47** 603
[5] Kwon J H *et al* 2010 Plasma density measurements by phase resolved cutoff *Appl. Phys. Lett.* **96** 081502
[6] Lapke M, Mussenbrock T and Brinkmann R P 2008 The multipole resonance probe: a concept for simultaneous determination of plasma density, electron temperature, and collision rate in low-pressure plasmas *Appl. Phys. Lett.* **93** 051502
[7] Dine S *et al* 2005 A novel technique for plasma density measurement using surface-wave transmission spectra *Plasma Sources Sci. Technol.* **14** 777–86
[8] Braithwaite N S, Sheridan T E and Boswell R W 2003 Transient RF self-bias in electropositive and electronegative plasmas *J. Phys. D: Appl. Phys.* **36** 2837–44
[9] Klick M, W Rehack and Kammeyer M 1997 Plasma diagnostics in RF discharges using nonlinear and resonance effects *Japan. J. Appl. Phys.* **36** 4625–31
[10] Walker D N, Fernsler R F, Blackwell D D and Amatucci W E 2006 On collisionless energy absorption in plasmas: theory and experiment in spherical geometry *Phys. Plasmas* **13** 032108
[11] Balmain K 1966 Impedance of a Spherical Probe in a Magnetoplasma *IEEE Trans. Antennas Propag.* **AP-14** 402
[12] Blackwell D D, Walker D N, Messer S J and Amatucci W E 2007 Antenna impedance measurements in a magnetized plasma: I. Spherical antenna *Phys. Plasmas* **14** 092105
[13] Piejak R B, Godyak V A, Garner R and Alexandrovich B M 2004 The hairpin resonator: a plasma density measuring technique revisited *J. Appl. Phys.* **95** 3785
[14] Boris D R, Walton S G, Baraket M and Fernsler R F 2010 Frequency probe measurements in electron beam generated plasmas *Proc. 53rd Society of Vacuum Coaters Technical Conf. (Orlando, FL)*
[15] Swanson D G 2003 *Plasma Waves* 2nd edn (Philadelphia, PA: Institute of Physics Publishing) p 24
[16] Bau S and Wendt A 1999 Sheath Thickness evaluation for collisionless or weakly collisional bounded plasmas *IEEE Trans. Plasma Sci.* **27** 1358
[17] Walker D N, Fernsler R F, Blackwell D D and Amatucci W E 2008 Determining electron temperature for small spherical probes from network analyzer measurements of complex impedance *Phys. Plasmas* **15** 123506

[18] Fernsler R F, Manheimer W M, Meger R A, Mathew J, Murphy D P, Pechacek R E and Gregor J A 1998 Production of large-area plasmas by electron beams *Phys. Plasmas* **5** 2137

[19] Manheimer W M, Fernsler R F, Lampe M and Meger R A 2000 Theoretical overview of the large-area plasma processing system (LAPPS) *Plasma Sources Sci. Technol.* **9** 370

[20] Lock E H , Fernsler R F and Walton S G 2008 Experimental and theoretical evaluations of electron temperature in continuous electron beam generated plasmas *Plasma Sources Sci. Technol.* **17** 025009

[21] Kanaya K, Ono S and Ishigaki F 1978 Secondary electron coefficients of insulators *J. Phys. D: Appl. Phys.* **11** 2425